ISSN 1063-7826, Semiconductors, 2012, Vol. 46, No. 9, pp. 1194–1200. © Pleiades Publishing, Ltd., 2012.
Original Russian Text © G.G. Untila, T.N. Kost, A.B. Chebotareva, M.B. Zaks, A.M. Sitnikov, O.I. Solodukha, M.Z. Shvarts, 2012, published in Fizika i Tekhnika Poluprovodnikov, 2012, Vol. 46, No. 9, pp. 1217–1223.

PHYSICS OF SEMICONDUCTOR DEVICES

# *n*-Si Bifacial Concentrator Solar Cell

**G. G. Untila[a]^, T. N. Kost[a], A. B. Chebotareva[a], M. B. Zaks[b], A. M. Sitnikov[b], O. I. Solodukha[b], and M. Z. Shvarts[c]**

[a] *Skobel'tsyn Research Institute of Nuclear Physics, Moscow State University, Moscow, 119991 Russia*
^ *e-mail: GUntila@mics.msu.su*
[b] *Solnechnyi Veter (Solar Wind) Limited-Liability Company, Krasnodar, 350063 Russia*
[c] *Ioffe Physical–Technical Institute, Russian Academy of Sciences, St. Petersburg, 194021 Russia*

Submitted February 27, 2012; accepted for publication, March 7, 2012

**Abstract**—Various approaches have been developed for reducing the cost of the photoelectricity produced by silicon solar cells (SCs). Of highest priority among these approaches are improvement of the efficiency of the SCs, transition from *p*-Si to *n*-Si, light concentration, and use of bifacial SCs. In the present study, an SC combining all these approaches has been developed. In this SC, transparent conducting oxides serve as antireflection and passivating electrodes in an indium–tin–oxide/($p^+nn^+$)-Si/indium–fluorine–oxide structure fabricated from Cz-Si with wire contacts (Laminated Grid Cell design). The SC has front/rear efficiencies of 16.5–16.7/15.1–15.3% X (under 1–3 suns). This result is unique because the combination of bifaciality and concentrator operation has no analogs and the SC compares well with the world standard among both bifacial and concentrator SCs.

**DOI:** 10.1134/S1063782612090229

## 1. INTRODUCTION

It is commonly accepted that, to reduce the cost of the electric power generated by solar cells (SCs) fabricated from crystalline silicon (*c*-Si), it is necessary to improve their efficiency and reduce their thickness [1] because more than half the cost of a solar module (SM) is constituted by the price of silicon wafers. It is preferable that SCs should possess three additional properties: be fabricated from *n*-type silicon, be bifacial, and be capable of operating in low-concentration systems. And why is this so?

### *1.1. Concentrator Photovoltaics (CPV)*

Light concentration with inexpensive lenses and reflectors improves power generation by photoelectric systems without making the area of high-cost SCs larger. However, although the concentrator approach has been the focus of interest of photovoltaics since the 1970s [2], it has still not fully realized its potential. Only ~20 MW of CPV systems were installed in the world by 2010 (<1% of the total volume) [3]. The cause of hindrance in CPV development is that inexpensive concentrator SCs could not be found on the market until very recently [4]. The high-concentration variant requires very precise complex tracking systems and high-efficiency high-concentration SCs whose manufacture requires expensive technologies. The higher the cost of an SC, the higher the concentration ratio $C$ required for its use to be economically justified. For example, the application of high-efficiency concentrator SCs (>26%) in an installation with a concentration ratio $C = 20–50$ X has been found to be uneconomical [5], because these SCs require $C > 100$ X.

Recently, a low-concentration variant combining simple inexpensive reflectors and ordinary silicon SCs adapted to a concentration ratio of $C = 2–5$ X has been under more active development [6, 7]. So far, standard SCs fabricated by the screen printing technique and improved by the electrolytic growth of contacts have a low efficiency: 14.0–15.5% at 1–14 X suns [8].

### *1.2. Bifaciality*

Bifacial SCs make it possible to raise the energy yield of photoelectric systems by utilizing light incident on the rear side by 11% [9], 21% [10], and in some cases, with proper installation, to 50% [11]. The advantage of bifacial SCs is fully exploited in concentrator systems. Compared with monofacial SCs of similar rated power, bifacial SCs produce a larger amount of energy, up to 10–20% in a concentrator system with $C = 1.6$ X [12] (because of the 12°C lower working temperature [13]) and up to 40% in a hybrid concentrator photoelectrothermal system [14].

In addition, some optical concentration systems, e.g., TRAXLE™ [15] or the unconventional low-cost Holographic Planar Concentrator™, which provides $C \approx 3$ X without a tracking system [16], are intended just for bifacial SCs.

### *1.3. n-Si*

*n*-Si SCs are preferable for two reasons. First, *n*-Si is less sensitive to common impurities (e.g., Fe [17]) and defects as compared with *p*-Si, and, therefore, the carrier lifetime and, accordingly, the maximum efficiency of these SCs are higher. Second, *n*-Si is stable, whereas SCs fabricated from boron-doped *p*-type Czochralski silicon (Cz-Si) are subject to light-induced degradation because of the formation of boron–oxygen complexes under the action of light, and their efficiency decreases in the course of time by ~1 abs % [18].

It is noteworthy that the dominant type of SCs manufactured satisfies none of these requirements: (i) it is fabricated from *p*-type silicon (by the screen printing technique); (ii) it is monofacial because its rear side is covered with a layer of aluminum paste; (iii) its efficiency is limited by strong recombination both in the heavily doped emitter, which is necessary for providing low resistance to the contacts, and at the metal-coated rear side; (iv) its thinning is precluded by the deformation of wafers during high-temperature firing of the pastes, which reduces the yield of the finished devices, especially in the case of thin wafers, and by strong recombination on the rear side; and, finally, (v) these SCs are unsuitable without additional modification for concentrator applications because of their high series resistance [19].

Thus, development of a high-efficiency bifacial concentrator SC based on *n*-type silicon with the use of simple low-temperature highly efficient metallization is the focus of the main areas of R & D in silicon photovoltaics. However, these areas are being developed in parallel. High-efficiency *n*-Si SCs are manufactured by the Sanyo company (HIT design, a heterojunction with an intrinsic thin layer) [9] and by the Sunpower and Amonix companies (IBC design, interdigitated back contact) [20]. HIT SCs are bifacial but not of concentrator type [21], and IBC SCs are of high concentration type, but monofacial and expensive, i.e., they are unsuitable for low-concentration systems [19].

Previously, we developed, based on the Laminated Grid Cell (LGCell) design and an indium–fluorine–oxide (IFO)/($n^+pp^+$)-Cz-Si/indium–tin–oxide (ITO) structure, bifacial concentrator *p*-Si SCs with front/rear efficiencies of 17.1–18.0%/13.3–13.6% at $C = 1–6$ X [22].

*n*-Si has been used to fabricate bifacial nonconcentrator SCs with front/rear efficiencies of 17.7/13.2% (front surface textured, rear surface smooth) [23] and with 16.3/14.5% for SCs with both surfaces being textured (confirmed at Sandia National Laboratories) [24].

The goal of our present study is to develop a bifacial *n*-Si SC to be used in low-concentration systems.

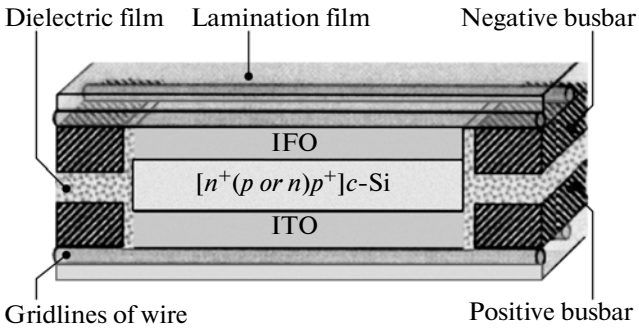


**Fig. 1.** Bifacial SC of the Laminated Grid Cell design with an IFO film on the $n^+$ surface, ITO film on the $p^+$ surface, and a wire contact grid; the busbars are situated near the SC.

## 2. EXPERIMENTAL PROCEDURE

To achieve this goal, we used the LGCell bifacial design (Fig. 1) with films of transparent conducting oxides (TCOs) as transparent, antireflection, and passivating electrodes and two (front and rear) wire grids, attached via a laminate film by the low-temperature (150°C) lamination method [25] to the TCOs and busbars situated near the structure. Also, a transparent conducting polymer material can be used [26].

We used 180-μm-thick 125 × 125 mm$^2$ *n*-Cz-Si (100) wafers (2 Ω cm) textured on both sides. ($p^+nn^+$) Cz-Si structures were fabricated by the diffusion of boron and phosphorus from deposited borosilicate and phosphosilicate glasses. After the glasses were removed in 4% HF, the surfaces of the structure were treated in a $HNO_3 : H_2O : HF$ etchant. As a result, the sheat resistance measured on the front surface ($p^+$-emitter) was 85 Ω/□, and on the rear surface, 30 Ω/□.

TCO films with a thickness of ~100 nm were deposited by the aerosol pyrolysis of a film-forming solution (FFS), produced by the ultrasonic method (pyrosol). The schematic of the installation for film deposition has been described previously [27]. Just before the deposition of the TCO, the structures were treated in a peroxide-ammonia solution (RCA cleaning technique: 10% $NH_4OH$ + 10% $H_2O_2$ in $H_2O$) and 4% HF.

First, an IFO film was deposited onto the rear $n^+$ surface from a solution of 0.2 M $InCl_3$ + 0.05 M $NH_4F$ + 0.1 M $H_2O$ in methanol at a temperature of 475°C, with Ar + 5% $O_2$ as the carrier gas [28]. The sheat resistance of the rear surface coated with IFO was 19 Ω/□.

Then, we deposited an ITO film onto the $p^+$ emitter from a solution of 0.1 M $InCl_3$ + 0.003 M $SnCl_4$ + XM $H_2O$ in methanol at a temperature of 375°C, with Ar as the carrier gas. The final sheat resistance of the front surface was 29 Ω/□.

After the TCO films were deposited, the wafers were cut into 20 × 20 mm$^2$ fragments with a diamond scriber. The front and rear contact grids fabricated from a copper wire 60 μm in diameter, coated with the

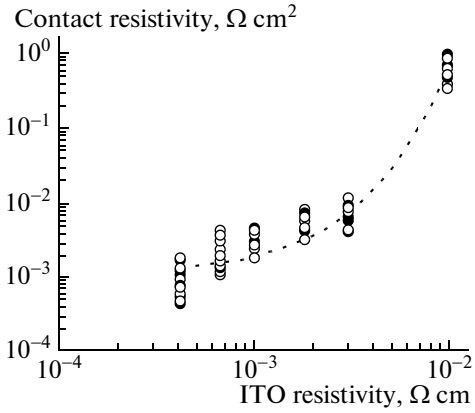


**Fig. 2.** Effect of the ITO film's resistivity on the specific resistance of the metal/ITO contact.

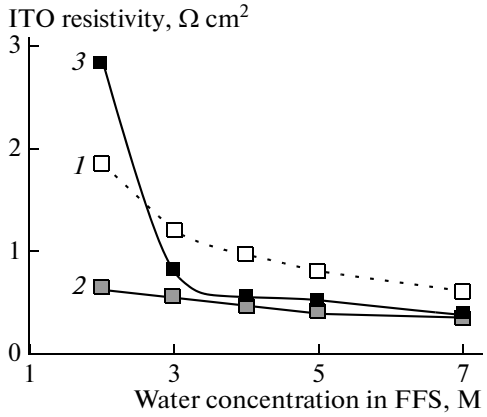


**Fig. 3.** Resistivity of the ITO films vs. the water concentration in the film-forming solution (FFS): (*1*) upon deposition, (*2*) after annealing, and (*3*) after eight months.

contact composition, were attached to the TCO films by lamination ($T \approx 150$°C). The spacing between the wires was 1.5 mm. The LGCell structure is shown schematically in Fig. 1. It is noteworthy that the interconnecting tabs are situated near the SC and do not shade it. In addition, a solder gun is not brought into contact with the silicon structure during subsequent soldering, which precludes any damage that possibly occurs in the case of conventional SCs.

To measure external quantum-efficiency spectra (*EQE*), we used a LOS-2 light source with a 1000-W xenon lamp and a set of interference light filters. The angle of beam incidence on the SC did not exceed 3°. A sample tested at Fraunhofer ISE laboratory was used for calibration. The SC photocurrent was found by multiplying the resulting *EQE* curve by the standard solar spectrum AM 1.5G 1000 W m$^{-2}$ (ASTM G173). The total-reflection spectra $R(\lambda)$ were measured with a LOMO-spectrum CF-56 spectrometer with an integrating sphere.

The concentration dependences of the LGCell SCs were studied at the Ioffe Physical–Technical Institute on a pulse simulator [29].

## 3. RESULTS AND DISCUSSION

### *3.1. Optimization of ITO Films*

Both surfaces of the bifacial SC LGCell ITO/($p^+nn^+$)-Cz-Si/IFO were covered with TCO films. To optimize the barrier properties of the TCO/Si contact [30], the deposition temperature should be rather high for the IFO film (475°C), and low for the ITO film (~400°C). Therefore, it is necessary to first deposit the IFO film, and then the ITO film. To avoid degradation of the IFO film's properties (in particular, its transparence) during ITO deposition, the ITO deposition temperature should be even lower (~380°C). However, lowering the deposition temperature of the ITO film leads to an increase in its resistivity $\rho_{ito}$ [31]. Accordingly, the series resistance of the SC increases due to an increase in the spreading resistance between the contact strips and to an increase in the resistance of the ITO/metal contact.

A special-purpose study by the ISCRA (Interface Specific Contact Resistance Analysis) method [32] revealed (Fig. 2) an increase in the specific resistance of the ITO/metal contact by three orders of magnitude, from <1 mΩ cm$^2$ to ~1 Ω cm$^2$, with the $\rho_{ito}$ increasing from 0.0004 to 0.01 Ω cm.

To make the $\rho_{ito}$ lower, we carried out a study that demonstrated (Fig. 3) that raising the concentration of water in the film-forming solution from 2 to 7 M reduces the $\rho_{ito}$ of the freshly deposited ITO films from ~2 mΩ cm$^2$ to 0.6 mΩ cm$^2$. Annealing of these films in argon with methanol vapor at 380°C for 10 min substantially, by more than a factor of 1.5, reduced the $\rho_{ito}$. However, the $\rho_{ito}$ of films obtained at a low water concentration (1 M) degraded as a result of aging (storage in air) to 3 mΩ cm$^2$, whereas films obtained at water concentrations of 4–7 M remained stable. Based on these results, we used a film-forming solution with 7 M of water to deposit the ITO films.

### *3.2. LGCell SC Parameters under 1-sun Illumination (1X)*

The spectra of external quantum efficiency *EQE* and reflectance *R* under front and rear illumination of an LGCell SC are shown in Fig. 4. The reflectances from the front and rear sides are about the same (5.5–7%) at wavelengths $\lambda$ = 700–900 nm. An important circumstance should be noted. The reflectance from the SC of the LGCell design is somewhat higher than that from ordinary high-efficiency SCs. The reason is that the LGCell is already laminated, i.e., it is covered with a lamination film that has a refractive index of

~1.56, and, therefore, the reflectance only from this film is about 5% in the whole spectral range.

Commonly, the values of parameters, including the reflectance spectra, are reported in published works for unencapsulated SCs whose reflectance can be close-to-zero in a certain spectral range (e.g., for a SunPower SC with rear-side contacts). However, this is only an apparent advantage because, in the end, all SCs in a module are covered with glass that has a refractive index of ~1.5, which leads to ~4% loss on reflection from the glass. Therefore, the parameters reported for the LGCell are to be considered extremely close to those in a module.

The maximum values of $EQE \approx 90\%$ at wavelengths $\lambda = 700$–$900$ nm under front illumination are limited from above by both reflection from the lamination film (~4.8%) and by shading by the wire contacts (~4.7%), which leads to a total decrease in *EQE* by ~9.5%. Consequently, the front and rear internal quantum efficiencies of the LGCell per active area at the peak of the *EQE* curve are ~99% and ~92%, respectively. The high values of the front and rear long-wavelength *EQE* (≥75% at $\lambda = 560$–$1000$ nm) indicate that the diffusion length of nonequilibrium carriers in the SC base is large and the effective recombination velocity on the rear $n^+$ surface generated by its etching and passivation with an IFO film is low.

By contrast, the comparatively low front short-wavelength *EQE* (48% at $\lambda = 400$ nm) indicates that the properties of the boron-doped $p^+$ emitter and its passivation by the ITO film are insufficiently optimized. A study of the profile of the boron-diffusion layer demonstrated that, even after this layer is etched, which raises its layer resistance to 85 Ω/□, the surface concentration of holes is rather high ($\geq 1 \times 10^{20}$ cm$^{-3}$ [33]) and this strongly reduces the lifetime of nonequilibrium carriers in the $p^+$ layer due to Auger recombination.

Table 1 lists the parameters of a bifacial concentrator LGCell SC, measured under 1-sun (1X) front and rear illumination. The bifaciality of this SC is 92% as regards both the photocurrent and efficiency. Such pronounced bifaciality became possible due to the high perfection of *n*-type silicon wafers (large diffusion length of minority carriers) and also the effective passivation of the rear surface by the $n^+$ layer and IFO film. Because the front and rear photocurrents have close values, the difference between the photovoltages (front and rear) is only 4 mV.

To assess the result obtained for the LGCell SC as a bifacial SC, we present data for bifacial SCs fabricated from Cz-Si of both *n*- and *p*-types (Table 2). It should be noted that these SCs are not of the concentrator type. The front/rear efficiencies of 16.5/15.1% under 1 sun, obtained in the present study for an LGCell SC based on *n*-Si, as well as the values of 17.7/13.3% for the bifacial LGCell based on *p*-Si, favorably compare with the best results, including even those for SCs fabricated with evaporated contacts ECO. Moreover, the LGCell SCs are of the concentrator type.

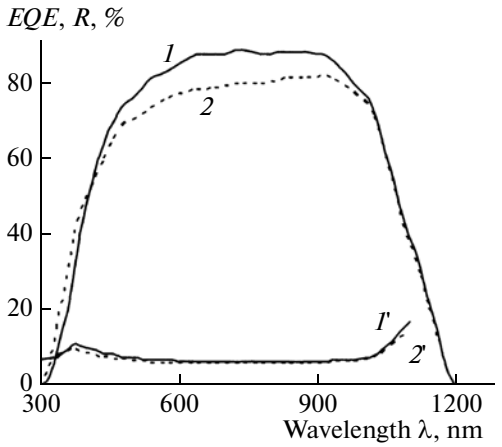


**Fig. 4.** Spectra of (*1*, *2*) external quantum efficiency *EQE* and (*1*', *2*') reflectance *R* under (*1*, *1*') front and (*2*, *2*') rear illumination of an SC.

These results need to be commented upon. It is known that the recombination at the unpassivated SC edge results in a decrease in all the SC parameters. The smaller the sample and the longer the lifetime τ of minority carriers in the base, the stronger the adverse influence of the edges. It has been shown experimentally that the SC efficiency approximately linearly decreases with increasing ratio between its perimeter *P* and area *S*, with a slope ratio whose value for front/rear illumination is 1.0/1.2 abs % for an SC with $\tau = 500$ μs and 0.4/0.5 abs % for $\tau = 100$ μs [34].

It is noteworthy that, as a rule, concentrator SCs are made smaller [45] than SCs intended for unconcentrated illumination. Consequently, because the $20 \times 20$ mm SC fabricated in the present study has $P/S = 2$ and long lifetime τ, it would be expected that an increase in size, e.g., to $125 \times 125$ mm ($P/S \approx 0.3$) could lead to a rise in its efficiency by 0.7–1.7 abs %. It should be added here that, for example, an efficiency of 15.2/17.7% was obtained in [35] on an SC

**Table 1.** ITO/($p^+nn^+$)-Cz-Si/IFO LGCell SC under 1-X front and rear illumination: efficiency (*Eff*), short-circuit current ($J_{sc}$), open-circuit voltage ($U_{oc}$), and fill factor (*FF*)

| Parameter | Front illumination | Rear illumination |
|---|---|---|
| *Eff*, % | 16.5 | 15.1 |
| $J_{sc}$, mA cm$^{-2}$ | 35.1 | 32.4 |
| $U_{oc}$, mV | 611 | 607 |
| *FF*, % | 76.7 | 76.7 |
| $R_s$, Ω cm$^2$ | 0.43 | |

**Table 2.** Efficiency of bifacial Cz-Si SCs under front and rear illumination

| Institution, details | *Eff*, % front_rear |
|---|---|
| *n*-type, Cz-Si | |
| IES-UPM, ECO 300 μm [35] | 15.2_17.7 |
| 140 μm [36] | 14.9_17.0 |
| 240 μm [36] | 14.2_14.9 |
| TiM-EHU, Isofoton, Fraunhofer. | |
| ISE, CENER, NPC, USF, Ferro. | |
| screen printing [37], 120 μm | 12.8_13.2 |
| 320 μm | 14.4_14.2 |
| ITM, Univ. Rais Vasco, screen | |
| printing, 120 μm [38] | 13.6_11.0 |
| Research Institute of Nuclear Physics, Solar Wind, concentrator LGCell | 16.5_15.1 |
| *p*-type, Cz-Si | |
| ISFH, screen print., 140 μm [39] | 14.6_13.0 |
| IES-UPM, ECO [37] 140 μm | 16.0_13.0 |
| 240 μm | 13.8_13.7 |
| ISC Konstanz, Univ. Stuttgart. | |
| screen print., selective BSF [40] | 15.9_14.1 |
| ISC Konstanz [41] | 16.4_14.4 |
| Aachen Univ., Deutsche Cell, | |
| Solland Solar, screen print. [42] | 17.0_10.3 |
| ISC Konstanz, screen print. [43] | 17.3_15.0 |
| Shanghai Univ., Georgia Inst. of | |
| Techn., Solarfun Co. [44] | 16.6_12.8 |
| Research Institute of Nuclear Physics, Solar Wind, concentrator LGCell [22] | 17.7_13.3 |

with no edges because of its formation as a mesa structure on a wafer 100 mm in diameter.

### *3.3. LGCell SC parameters under Concentrated Illumination*

The variation in the conversion parameters of our bifacial LGCell SC with increasing concentration ratio $C$ under front illumination is shown in Fig. 5.

In the optimal range of light concentration ratios (1–3) X, the front efficiency varies from 16.5 to 16.7% (rear efficiency, from 15.1 to 15.3%). The efficiency continues to increase as the illumination is increased to $C \sim 2.5$ X. The value of $U_{oc}$ steadily increases with the concentration ratio $C$ by the logarithmic law, $U_{oc} = U_{oc}(C = 1) + (nk_BT/e)\ln(C)$, where $n$ is the ideality factor of the diode structure, found to be close to unity ($n = 1.08$); $k_B$ is the Boltzmann constant; $T$ is the temperature (K); and $e$ is the elementary charge.

The fill factor $FF$ decreases with increasing $C$ due to series resistance $R_s$ (Fig. 5). It should be noted that this resistance decreases with increasing illumination, which is, as a rule, observed in concentrator SCs and is associated with a decrease in the base resistance due to modulation by the photoconductivity effect and, possibly, with nonlinearity of the contact resistances. The optimal concentration ratio $C_{opt}$, at which the efficiency is the highest, is $C_{opt} \approx 2.5$, and the resistance at this point is $R_s \approx 0.4\ \Omega\ cm^2$, i.e., the law $C_{opt} \propto 1/R_s$ is observed.

As regards the value of $R_s$ for our LGCell SC, the following circumstance should be noted. The SC efficiency is commonly raised by using high-efficiency diffusion layers with a high sheat resistance, produced by various methods, including etch-back [46]. In the LGCell SC, the etch-back of both the front [23] and rear [47] diffusion layers also led to an increase in efficiency. In the present study, the sheat resistance of the front/rear surfaces was brought to 85/30 Ω/□ by etching. In the case of a bifacial SC with a dielectric antireflection coating and screen-printed contacts with a spacing of 2–2.5 mm between the contact gridlines, only spreading between the gridlines would yield a contribution to $R_s = 0.4$–$0.6\ \Omega\ cm^2$. However, owing to the use of IFO and ITO films in the LGCell design, which reduce the sheat resistances of the front/rear surfaces to 29/19 Ω/□, and thanks to the thinner wire contacts, which make it possible to reduce the distance between these contacts to 1.5 mm at the same shading, this component of $R_s$ could be reduced by a factor of 4–6, to ~$0.09\ \Omega\ cm^2$. One more note should be made: one of the $R_s$ components inherent in SCs with TCO films is the poorly studied resistance of the TCO/Si contact. However, in the case of the IFO/$n^+$-Si contact, this resistance may be noticeable [48], and, in all probability, just this component can significantly contribute to $R_s$. Thus, the contact system of the LGCell design enabled the fabrication of a high-efficiency SC that is not only bifacial, but also is of the concentrator type.

To assess the resulting LGCell SC as that of the concentrator type, we present for comparison the data reported in 2011 by the Narec company [44], which specializes in the development and manufacture of monofacial concentrator SCs and fabricates these cells by the laser-grooved-buried-contact (LGBC) technique from $p$-type silicon. The LGBC concentrator SCs produced by Narec demonstrated an efficiency of 17.0–17.1% under 4–10 suns. However, these results were obtained for a monofacial SC, which was, in addition, fabricated from degradable $p$-type silicon.

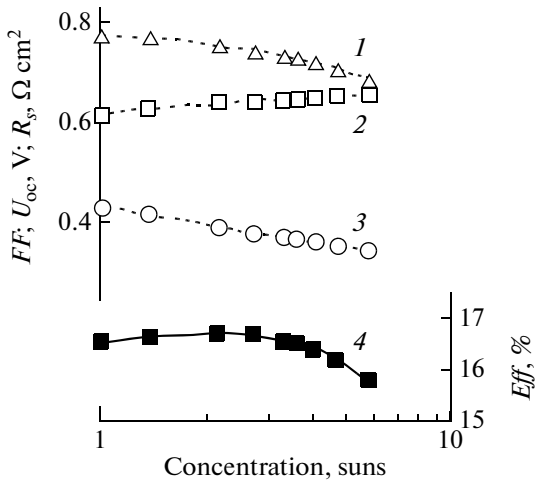


**Fig. 5.** Variation in the front parameters of a bifacial LGCell SC based on the ITO/($p^+nn^+$)-Cz-Si/IFO structure with increasing illumination: (*1*) *FF*, (*2*) open-circuit voltage $U_{oc}$, (*3*) series resistance $R_s$, and (*4*) efficiency *Eff*.

## 4. CONCLUSIONS

In this study, due to the application of the Laminated Grid Cell design, a concentrator bifacial solar cell (SC) with an ITO/($p^+nn^+$)-Cz-Si/IFO structure was fabricated from conventional *n*-type Czochralski silicon. The SC demonstrated front/rear efficiencies of 16.5–16.7/15.1–15.3% under illumination of 1–3 suns. This result is unique because the LGCell obtained compares well with the world standard in, first, the class of bifacial SCs and, second, in the class of concentrator SCs. Analysis of the relevant published works shows that no reports about the development of bifacial concentrator SCs have been made thus far.

A conclusion was made, based on an analysis of the SC parameters, that a further increase in efficiency requires the solution of problems associated with (i) recombination in the $p^+$ layer and passivation of this layer, (ii) recombination at cell edges, and (iii) resistance of the IFO/$n^+$-Si contact.

## ACKNOWLEDGMENTS

The study was supported by a grant for leading scientific schools (NSh-3322.2010.2) and by the Russian Foundation for Basic Research (grant nos. 10-08-01171, 10-08-00737, 11-08-01301, 11-08-01251).

## REFERENCES

1. S. W. Glunz, Solar Energy Mater. Solar Cells **90**, 3276 (2006).
2. R. M. Swanson, Progr. Photovolt.: Res. Appl. **8**, 93 (2000).
3. F. Rubio, M. Martinez, A. Hipolito, A. Martin, and P. Banda, in *Proceedings of the 25th European Photovoltaic Solar Energy Conference* (Valencia, 2010), p. 1008.
4. M. Castro, I. Anton, and G. Sala, Solar Energy Mater. Solar Cells **92**, 1967 (2008).
5. A. W. Blackers, in *Proceedings of the 16th European Photovoltaic Solar Energy Conference* (Glasgow, 2000).
6. B. A. Butler, E. E. vanDyk, F. J. Vorster, W. Okullo, M. K. Munji, and P. Booysen, Physica B (2011). doi:10.1016/j.physb.2011.09.071 (2011).
7. L. M. Fraas, J. E. Avery, H. X. Huang, L. Minkin, J. X. Fraas, L. C. Maxey, and A. Gehl, in *Proceedings of the 33rd IEEE Photovoltaic Special Conference* (San Diego, 2010), 978-1-4244-1641-7/08.
8. J. Coello, M. Castro, O. Anton, G. Sala, and M. A. Vazzquez, Progr. Photovolt.: Res. Appl. **12**, 323 (2004).
9. T. Mishima, M. Taguchi, H. Sakata, and E. Maruyama, Solar Energy Mater. Solar Cells **95**, 18 (2011).
10. L. Krenin, N. Bordin, A. Karsenty, A. Drori, and N. Eisenberg, in *Proceedings of the 26th European Photovoltaic Solar Energy Conference* (Hamburg, 2011), p. 3140.
11. A. Cuevas, A. Luque, J. Equren, and J. Del Alamo, Sol. Energy **29**, 419 (1982).
12. M. Libra and V. Poulek, in *Proceedings of the 19th European Photovoltaic Solar Energy Conference* (Paris, 2004), p. 2430.
13. http://www.solar.-trackers.com/bifacial-solar-panels
14. B. Robles-Ocampo, E. Ruiz-Vasquez, H. Canseco-Sanchez, R. C. Cornejo-Mezac, G. Trapaga-Martinez, F. J. Garcıa-Rodrigueza, J. Gonzalez-Hernandez, and Yu. V. Vorobiev, Solar Energy Mater. Solar Cells **91**, 1966 (2007).
15. M. Libra, V. Poulek, and J. Mares, in *Proceedings of the 23rd European Photovoltaic Solar Energy Conference* (Valencia, 2008), p. 926.
16. http://prismsolar.com/homepage.html.
17. D. Macdonald and L. J. Geerligs, Appl. Phys. Lett. **85**, 4061 (2004).
18. K. Bothe and J. Schmidt, in *Proceedings of the 20th European Photovoltaic Solar Energy Conference* (Barselona, 2005), p. 757.
19. M. Vivar, C. Morilla, I. Anton, J. M. Fernandez, and G. Sala, Solar Energy Mater. Solar Cells **94**, 187 (2010).
20. E. VanKerschaver and G. Beaucarne, Progr. Photovolt.: Res. Appl. **14**, 3107 (2006).
21. Q. Wang, M. R. Page, E. Iwaniczko, Y.-Q. Xu, L. Roybal, A. Duda, F. Hasoon, S. Ward, D. Wang, and P. R. Yu, in *Proceedings of the 25th European Photovoltaic Solar Energy Conference* (Valencia, 2010), p. 1295.
22. T. Kost, G. Untila, A. Chebotareva, M. Zaks, A. Sitnikov, O. Solodukha, and M. Shvarts, in *Proceedings of the 25th European Photovoltaic Solar Energy Conference* (Valencia, 2010), p. 2588.
23. G. Untila, A. Osipov, T. Kost, A. Chebotareva, M. Zaks, A. Sitnikov, and O. Solodukha, in *Proceedings of the 17th European Photovoltaic Solar Energy Conference* (Munich, 2001), p. 1796.
24. G. Untila, A. Osipov, T. Kost, A. Chebotareva, M. Zaks, A. Sitnikov, O. Solodukha, and A. Pinov, in *Proceedings of the 17th European Photovoltaic Solar Energy Conference* (Munich, 2001), p. 1793.

25. G. G. Untila, T. N. Kost, A. B. Chebotareva, M. B. Zaks, A. M. Sitnikov, and O. I. Solodukha, Semiconductors **39**, 1349 (2005).
26. A. Chebotareva, G. Untila, T. Kost, A. Lachinov, V. Kornilov, and S. Salazkin, in *Proceedings of the 21st European Photovoltaic Solar Energy Conference* (Dresden, 2006), p. 291.
27. A. Chebotareva, G. Untila, and T. Kost, Thin Solid Films **515**, 8505 (2007).
28. G. G. Untila, T. N. Kost, and A. B. Chebotareva, Thin Solid Films **518**, 1345 (2009).
29. M. Z. Shvarts, V. D. Rumyantsev, V. M. Andreev, V. R. Larionov, and D. A. Malevskiy, in *Proceedings of the 4th Conference on Solar Concentrators for the Generation of Electricity or Hydrogen* (El Escorial, 2007), p. 277.
30. G. Untila, T. Kost, A. Chebotareva, M. Zaks, A. Sitnikov, and O. Solodukha, in *Proceedings of the 21st European Photovoltaic Solar Energy Conference* (Dresden, 2006), p. 1199.
31. G. G. Untila, T. N. Kost, A. B. Chebotareva, M. B. Zaks, A. M. Sitnikov, and O. I. Solodukha, Semiconductors **42**, 406 (2008).
32. G. Untila, A. Osipov, T. Kost, and A. Chebotareva, in *Proceedings of the 17th European Photovoltaic Solar Energy Conference* (Munich, 2001), p. 265.
33. G. G. Untila, T. N. Kost, A. B. Chebotareva, M. B. Zaks, A. M. Sitnikov, and O. I. Solodukha, Semiconductors **46**, 832 (2012).
34. G. Untila, A. Chebotareva, T. Kost, A. Sitnikov, and O. Solodukha, in *Proceedings of the 20th European Photovoltaic Solar Energy Conference* (Barselona, 2005), p. 1255.
35. C. delCanizo, A. Moehlecke, I. Zanesco, I. Tovias, and A. Luque, IEEE Trans. Electron. Dev. **48**, 2337 (2001).
36. A. C. Pan, D. delCanizo, and A. Laque, in *Proceedings of the 22nd European Photovoltaic Solar Energy Conference* (Milan, 2007), p. 1438.
37. J. C. Jimeno, G. Bueno, R. Lago, I. Freire, L. Pérez, F. Recart, I. Hoces, N. Azkona, J. Alonso, P. Sánchez-Friera, S. W. Glunz, G. Emanuel, R. Ruiz, A. Pohl, W. Wolke, M. Schubert, I. Gavilanes, M. Gavilanes, M. Ezker, A. Turumbay, H. Sato, J. Bragagnolo, P. M. Nasch, S. Ostapenko, A. Belyaev, W. Dallas, O. Polupan, K. Albertsen, A. Shaikh, H. Kerp, and J. Salami, in *Proceedings of the 22nd European Photovoltaic Solar Energy Conference* (Milan, 2007), p. 875.
38. I. Hoces, N. Azkona, L. Perez, F. Recart, and J. C. Jimeno, in *Proceedings of the 25th European Photovoltaic Solar Energy Conference* (Valencia, 2010), p. 1974.
39. S. Steckemetz, A. Metz, and R. Hein, in *Proceedings of the 17th European Photovoltaic Solar Energy Conference* (Munich, 2001), p. 1902.
40. C. Duran, S. J. Eisele, T. Buck, R. Kopecek, J. R. Kohler, and J. H. Werner, in *Proceedings of the 24th European Photovoltaic Solar Energy Conference* (Hamburg, 2009), p. 1775.
41. S. Gloger, S. Riegel, B. Raabe, and G. Hahn, in *Proceedings of the 24th European Photovoltaic Solar Energy Conference* (Hamburg, 2009), p. 1544.
42. L. Janssen, H. Windgassen, D. L. Batzner, B. Bitnar, and H. Heuhaus, Solar Energy Mater. Solar Cells **93**, 1435 (2009).
43. C. Duran, T. Buck, R. Kopecek, J. Libal, and F. Traverso, in *Proceedings of the 25th European Photovoltaic Solar Energy Conference* (Valencia, 2010), p. 2348.
44. L. Yang, Q. H. Ye, A. Ebong, W. T. Song, G. J. Zhang, J. X. Wang, and Y. Ma, Progr. Photovolt.: Res. Appl. **19**, 275 (2011).
45. K. Drew. L. M. Brown, A. Cole, K. C. Heasman, and T. M. Bruton, in *Proceedings of the 26th European Photovoltaic Solar Energy Conference* (Hamburg, 2011), p. 625.
46. B. Raabe, F. Book, A. Dastgheib-Shirazi, and G. Hahn, in *Proceedings of the 25th European Photovoltaic Solar Energy Conference* (Valencia, 2010)p. 1174.
47. G. Untila, T. Kost, A. Chebotareva, M. Zaks, A. Sitnikov, and O. Solodukha, in *Proceedings of the 21nd European Photovoltaic Solar Energy Conference* (Dresden, 2006), p. 1258.
48. G. Untila, T. Kost, A. Chebotareva, M. Zaks, A. Sitnikov, and O. Solodukha, in *Proceedings of the 22nd European Photovoltaic Solar Energy Conference* (Milan, 2007), p. 600.

*Translated by M. Tagirdzhanov*